Desalination and Water Treatment
www.deswater.com

doi: 10.5004/dwt.2021.27427

230 (2021) 400–410
August

Fenitrothion pesticide adsorption from aqueous solution using copper nanopar-ticles modified 13X zeolite

Hossein Esfandian

Faculty of Engineering Technologies, Amol University of Special Modern Technologies, Amol, Iran, email: Hossein.Esfandian@gmail.com

Received 5 December 2020; Accepted 14 May 2021

ABSTRACT

In this study, the modified 13X zeolite by copper nanoparticles (copper nanoparticles were coated on a bed of 13X), was used as an adsorbent for adsorption of fenitrothion from aqueous solutions in a batch process. The results indicated that the maximum adsorption rate was 97% (with values of 6, 0.2 g, 20 min, and 20°C for pH, adsorbent mass, contact time, and temperature respectively). Kinetic studies showed that the pesticide adsorption process could be well described using the pseudo-second-order (Type 1) kinetic model. Langmuir-Type 1 isotherm, as well, covers the equilibrium data with a maximum absorption capacity of 63.29 mg/g for modified 13X. The results of the tests showed that the temperature increase has a negative effect on the removal efficiency. The thermodynamic parameters showed that the adsorption of fenitrothion pesticide on modified 13X in the studied conditions was spontaneous and exothermic.

Keyword: Zeolite; Fenitrothion; Modified 13X; Nanoparticles

1. Introduction

The presence of pesticides in soils, groundwater, and surface water is currently an important concern throughout the world because many of these materials are harmful to both human health and the environment. The increasing application of pesticides in agriculture fields for controlling pests is polluting water resources every day [1,2]. The pesticides are mostly non-biodegradable water pollutants and pesticides are carcinogenic in nature. So toxicity of pesticides and their products after degradation is making these compounds a high-potential hazard by contaminating the environment [2]. Applied pesticides may transfer into water sources based on direct washing and irrigation [3,4]. Fenitrothion is a kind of organophosphate pesticide. Volatile insecticides are also greatly used to remove flies and ticks, especially O. tholozani tick [5–10]. Pesticide's harmful effects on human health and the environment significantly depend on chemical material type, duration, exposure time, input concentration, and the amount of venom, [11,12]. Many research demonstrated that pesticides are the reason for abortion, mental retardation, teratology effects, and some defects in body tissues and actions. Organophosphate toxins like fenitrothion have an effect on acetylcholinesterase and lead to severe nervous side effects [8,10]. Meanwhile, fenitrothion is easily absorbed into the skin and holds a synergic characteristic with other toxins like pyrethrins [13].

The European Union determined a maximum allowed concentration of 0.5 μg/L for the combination of all pesticides and 0.1 μg/L for individual compounds in drinking water [14].

Different methods like adsorption processes [15,16], advanced oxidation processes including Fenton [17], photo-Fenton [18], UV/H_2O_2 [19,20], UV/TiO_2 [21–23], and anodic Fenton [24,25] were used to eliminate pesticides from water and wastewater. Adsorption shows one of the most suitable methods for the elimination of pollutants from the environment. It is a means of limiting the mobility of pollutants to a wider area once they get adsorbed

[26–28]. Different types of sorbents were investigated for the removal of fenitrothion from the water and wastewater such as agricultural soil [29], surfactant modified agricultural soil [30], organo-zeolites [31], and modified montmorillonite [32].

Zeolites like type X zeolites are mostly used as adsorbents. The type X zeolites framework is the same as naturally occurring faujasites and they are the large pore zeolites among any other known zeolites. Na^+ as the major alkaline cation and a 13.7 Å free diameter of the central cavity are the characteristics of 13X zeolites. Approximately 7.4 Å 12-member oxygen ring apertures allow for the transfer of molecules with a kinetic diameter of 8.1 Å [33,34]. Thus, zeolite 13X are good sorbents for pesticide adsorption. The purpose of this study was to investigate the process of fenitrothion pesticide adsorption from an aqueous solution by modified 13X. These experiments were performed on a batch system. The effect of experimental parameters of contact time, adsorbent dosage, initial fenitrothion concentration, and temperature on adsorption was studied. Finally, some isotherm and kinetic models have been used to study absorption. The thermodynamics of the fenitrothion adsorption process from an aqueous solution by modified 13X has been investigated.

2. Materials and methods

2.1. Reagents and chemicals

Copper nanoparticles (60–80 nm) and fenitrothion pesticide (95%–96% active substance) were prepared from Sigma-Aldrich Company, (Germany) and X13 zeolite with the purity of more than 90% was purchased from Iran Zeolite Company, (Tehran, Iran). Also $Cu(NO_3)_2$ was prepared by Merck Company, (Germany) was also used. Different concentrations of fenitrothion in the range of 50–225 mg/L were prepared from the stock solution using doubly distilled water. pH of the solution was adjusted to 6 by adding H_2SO_4 (1 M) and NaOH (1 M). UV-Vis spectrophotometry technique (T90+ UV/Vis Spectrophotometer PG Instruments Ltd) analysis at the maximum wavelength (λ_{max}) 271 nm [4,35] was used for the determination of the concentration of fenitrothion solution.

2.2. Instrumentation

The characterization of raw and modified 13X was investigated by the X-ray diffraction (XRD) patterns in a scan range of 10–70. Besides, Fourier-transform infrared (FTIR) (Shimadzu 4100, Japan) was performed in order to determine the functional groups of 13X zeolite before and after modification in the range of 400–4,000 cm^{-1}. The specific surface area and pore size distribution were determined using the Brunauer–Emmett–Teller (BET) and Barrett–Joyner–Halenda method respectively based on measuring the volume of nitrogen gas adsorption and desorption by the surface of the material at a constant liquid nitrogen temperature (77 K). The scanning electron microscope (SEM) device (Model S3400, Hitachi, Japan) was used to identify the surface of zeolites. Also, energy-dispersive X-ray (EDX) spectra were carried out on an EDX Genesis XM2 attached to SEM.

2.3. Batch adsorption experiments

Adsorption experiments were performed in batch mode (at a constant temperature of 20°C on a magnetic mixer at 400 rpm). In each experiment, the pH of the solution was adjusted by pH meter and using H_2SO_4 (1 M) and NaOH (1 M). After each test, the solution was filtered using a centrifuge and the sample was prepared for analysis and determination of the concentration of fenitrothion. Each experiment was repeated duplicate and its results were compared to each other without making mistakes. The experimental test error was below 5%. The fenitrothion removal efficiency in each experiment can be determined using the Eq. (1):

$$\%\text{Removal} = \frac{\left(C_i - C_e\right)}{C_i} \times 100 \tag{1}$$

where C_i and C_f are the initial concentration (mg/L) and the final concentration (mg/L) respectively. The fenitrothion sorption capacity by modified 13X at the time was calculated as follows:

$$q_t = \left(C_i - C_t\right) \times \frac{V}{m} \tag{2}$$

where q_t (mg/g) is the amount of adsorbed fenitrothion at time t; V (L) and C_t (mg/L) are the volume of solution and fenitrothion concentrations at time t, respectively; and m is the amount of adsorbent (g).

The amount of exchanged fenitrothion ion, q_e (mg/g) was obtained as Eq. (3):

$$q_e = \left(C_e - C_t\right) \times \frac{V}{m} \tag{3}$$

where C_e (mg/L) is the concentration of fenitrothion ion at equilibrium.

2.4. Synthesis of Cu modified 13X

In the first step, 10 g of raw zeolite was stirred in 150 mL distilled water for 1 h and then the mixture was placed in a stationary state for 20 min. Finally, the suspension was filtered. This operation was repeated several times. In the next step, the resultant was stirred for 24 h in 200 mL of 0.1 M $Cu(NO_3)_2$ solution under magnetic stirring (400 rpm). Then, the mixture was centrifuged, washed with deionized water and dried using an oven at 103°C. For coating of nanoparticles on the zeolite, 0.1 g of copper nanoparticles (60–80 nm) was poured in 30 mL of distilled water and sonicated for 15 min. Then, 6 g of prepared zeolite in the previous step was added to the copper nanoparticle suspension and shook moderately for 2 h. Finally, the resulting mixture was dried slowly at 80°C for 24 h the products were passed through a sieve shaker after drying. The added value of copper nanoparticles was such that it was 3 wt.% of 13X zeolite.

3. Results and discussion

3.1. Characterization of 13X zeolite

The raw and modified 13X were characterized using XRD, SEM, EDX and FTIR. Fig. 1a and b indicate that the XRD powder pattern of raw and modified 13X zeolite. The results revealed that all 13X zeolite characteristic peaks exhibited at 2θ values of 10°, 11.6°, 15.4°, 20°, 23.3°, 26.7°, 29.3° and 31° which were all presented to the typical pattern of crystalline 13X zeolite [36,37]. The XRD of modified 13X (with copper nanoparticles), indicates that no significant metal oxide peaks are found in the profiles of 13X zeolite, which may be attributed to the uniform dispersion of metal nanoparticles on 13X zeolite. The SEM image of the zeolite 13X (raw and modified zeolite) is indicated in Fig. 2a and b. As can be seen, zeolite has a

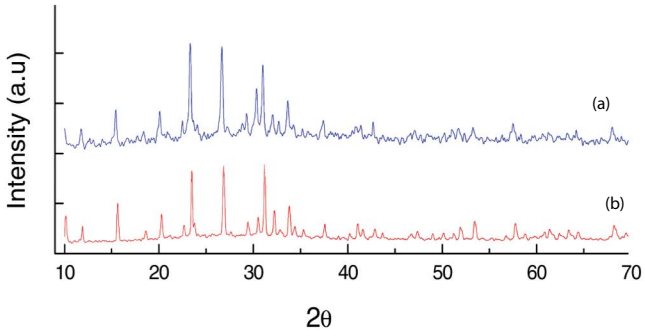

Fig. 1. X-ray diffraction of 13X zeolite (a) raw zeolite and (b) Cu modified zeolite.

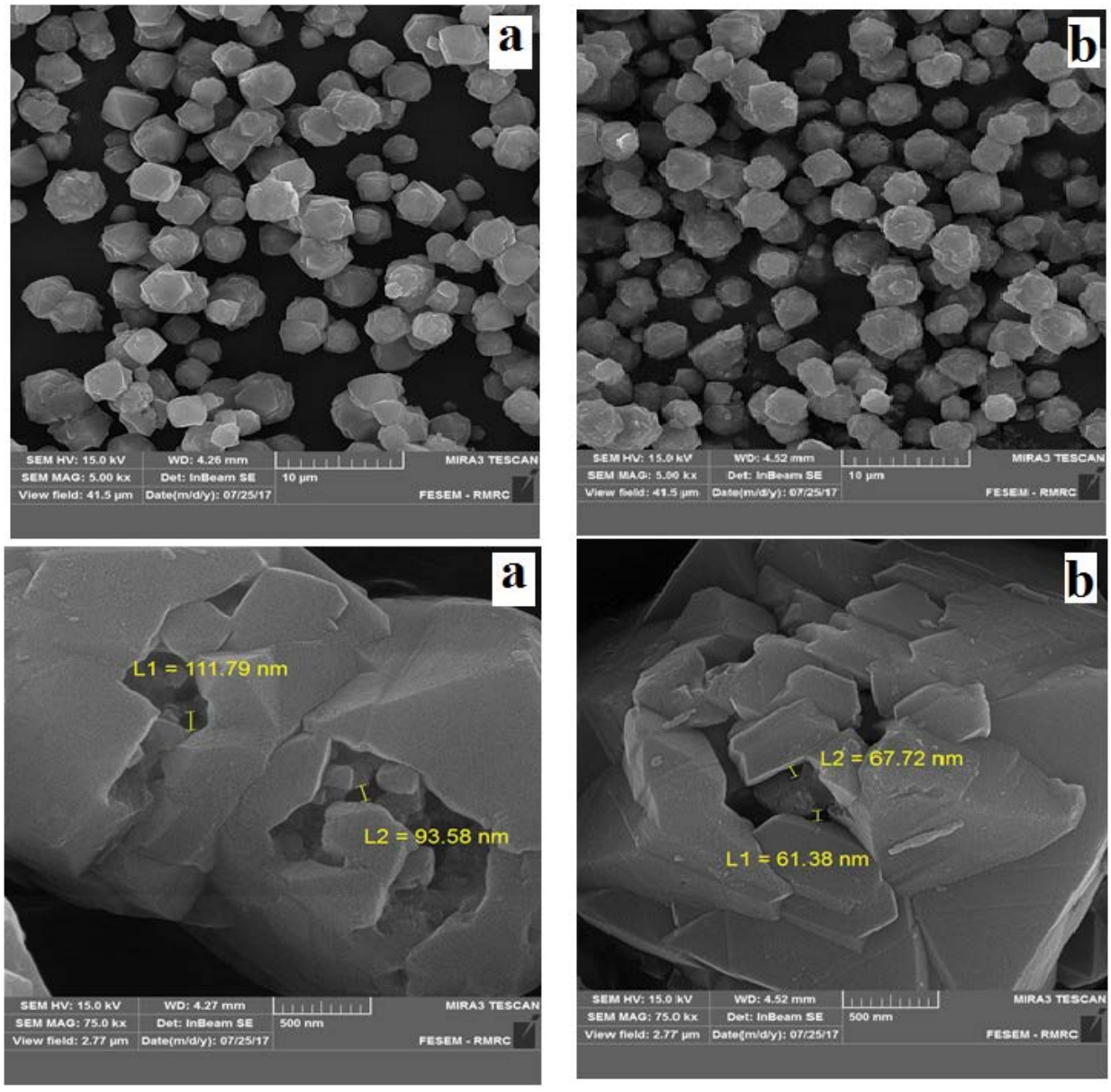

Fig. 2. Scanning electron micrographs (SEM) image of 13X zeolite (a) raw zeolite and (b) Cu modified zeolite.

spherical, regular and crystalline structure with an average diameter of 90–120 nm which is preserved after the loading of nanoparticles. The EDX to determine the elemental analysis of raw and modified 13X is presented in Fig. 3. Table 1 shows the EDX analysis results (amounts of elements) for raw and modified zeolite. The 13X zeolite was examined before and after modification for obtaining vibrational information about the species in materials by the FTIR spectroscopy device. Therefore, the wavelength, chemical bond, and bond type of raw and modified zeolite by copper in the 400–4,000 cm^{-1} range are indicated in Fig. 4. The band located at 420–500 cm^{-1} corresponding

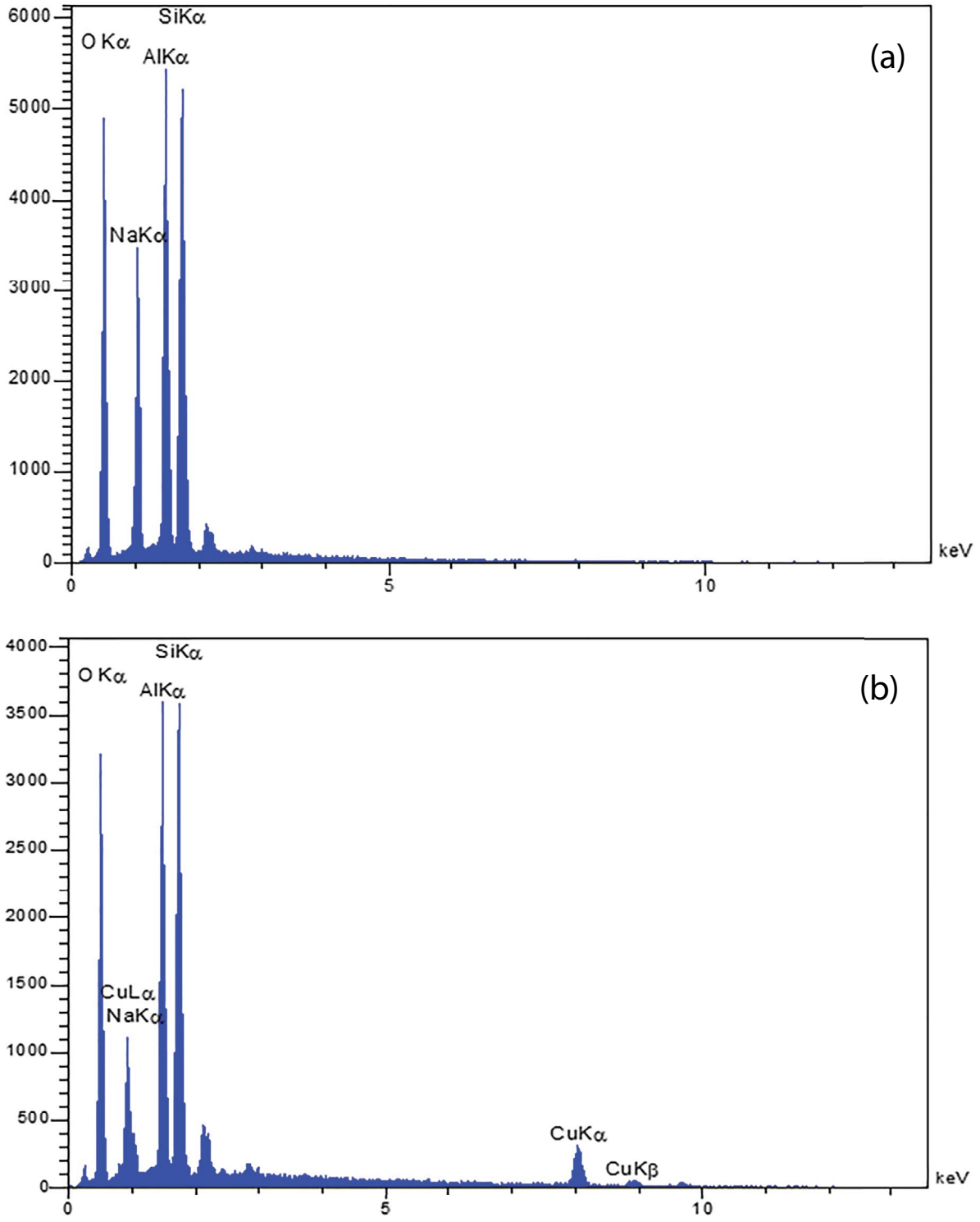

Fig. 3. EDX spectrum of 13X zeolite (a) raw zeolite and (b) Cu modified zeolite.

Table 1
Amounts of the elements obtained by EDX analysis

Raw 13X		Modified 13X
Element	wt.%	wt.%
O	51.08	46.35
Na	13.61	2.20
Al	16.62	15.68
Si	18.70	17.54
Cu	–	18.23
Total	100	100

to quadrilateral internal vibrations (vibrations of lattice atoms) and flexural oscillations O–Si–O and Si–O–Si, the peak at 500–650 cm^{-1} is ascribed to the elated to the external vibrations of the zeolite frame (external connections) and the presence of interlocking rings (double chain) in the zeolite structure, the vibrations of lattice atoms and symmetric tensile is shown at 650–730 cm^{-1}, the strong broadband at 950–1,250 cm^{-1} is related to the T–O band (T = silica or aluminum) and its sharpness indicates the quadrilateral internal vibrations and asymmetric tensile oscillations. The peak at 1,050–1,150 cm^{-1} is ascribed to the external vibrations of the zeolite frame (external joints) and asymmetric tensile vibrations. The strong broadband at 3,520–3,630 cm^{-1} (centered at 3,740 cm^{-1}) is represented using the stretching of water molecules adsorbed on OH groups [38–40]. The N_2 adsorption–desorption isotherms and pore size distributions of 13X zeolite (raw and modified zeolite) are presented in Fig. 5. The results indicate that the N_2 adsorption–desorption isotherms of modified and raw 13X zeolite are Type III of the International Union of Pure and Applied Chemistry classification. Results show that the amount of adsorbed N_2 is decreased with the impregnation of nanoparticles on a bed of 13X, which is due to the blockage of the pores, especially at the micropores [41]. The BET results (Table 2) indicated that the micropore surface area and micropore volumes modified 13X are decreased from the raw 13X zeolite, whereas, the external surface area is almost constant.

3.2. Effect of contact time and pH

Fig. 6 shows the effect of the contact time on the fenitrothion removal efficiency by modified 13X. For these experiments, the initial concentration of fenitrothion in aqueous solution (100 mL), pH, adsorbent dosage, and temperature were 50 mg/L, 6, 0.2 g, and 20°C respectively. As shown in Fig. 6, the pesticide removal efficiency from the aqueous solution was reached the maximum value after 20 min and then very little change in removal efficiency is observed. According to these results, the optimized contact time for fenitrothion sorption was determined 20 min on modified 13X.

To investigate the effect of the initial pH on the fenitrothion ions removal, some experiments were carried out at different initial pHs in the range of 2–9 at room temperature (i.e., 20°C) for 20 min (Fig. 7). As can be observed, increasing pH leads to an increase in the fenitrothion removal efficiency and it later reaches a maximum value at pH 6 and then decreases for modified 13X. The pH_{pzc} value for the modified 13X zeolite was found between the 7–8 pH range which indicates that the adsorbent surface was negatively charged at pH > pH_{pzc} and become positively charged at pH < pH_{pzc} and this will help in better adsorptive removal [42]. It can be concluded that at a pH value less than the value of point of zero charges, the adsorbent surface becomes positively charged which leads to greater electrostatic interaction for fenitrothion sorption [43].

3.3. Kinetics of sorption

Many absorption phenomena are dependent on time with different adsorbents. To understand the dynamics of the reaction and to predict the rate of absorption with time, knowing the kinetics of these processes is very important. Several kinetic models are used for absorbance in discontinuous processes, but due to the mathematical complexity of these models, they cannot be easily applied. In this regard, reactions that change q_t based on time can be simplified and easier for the kinetics of absorption. Models used in this field are Morris–Weber, pseudo-first-order kinetic and pseudo-second-order models. Of course, in the pseudo-first-order equations, it is assumed that the difference between q_t and q_e is the main propulsion force for the absorption action, and the adsorption rate is proportional to this force. To investigate the influence of penetration in the kinetics of the process, the Morris–Weber equation is used. The process of adsorption of particles from an aqueous solution onto the adsorbent occurs in several steps, where the total absorption process may be controlled by one or more of these steps. The first step involves the penetration of the absorbing material from the solution to the external surface of the absorbent. The penetration of the cavity is the second stage, and if this is a controlling step, this phenomenon can be studied using the Morris–Weber equation. The third stage is penetration at the absorbent level. The third stage generally states that the final equilibrium is based on the very low concentration of absorbed material in solution and the loss of active sites in the adsorbent [44]. The first step involves the penetration of the absorbing material from the solution to the external surface of the absorbent, the penetration of the cavity, which is the second stage, which, if this stage is controlling, can be studied using the Morris–Weber equation. The third stage is the penetration of the absorbent surface. In general, the third step states that the final equilibrium is due to the very low concentration of absorbed material in solubilization and the loss of active sites in the adsorbent for absorption action. In this study, the sorption kinetic data for fenitrothion sorption onto modified 13X adsorbent were analyzed using different kinetic models such as Morris–Weber, pseudo-first-order kinetic and pseudo-second-order Types 1-4 models. The details of the kinetic models were completely described in our previous study [43,45]. Kinetic results are indicated that in Table 3. As can be seen, the pseudo-second-order type-1 equation offers the best correlation which indicates that the rate-limiting step in the fenitrothion uptake process is the chemical sorption reaction involving the exchange of the electrons between adsorbent and adsorbate. The pseudo-first-order is dominant for the kinetic of adsorption process for the high concentration of pollutants whereas

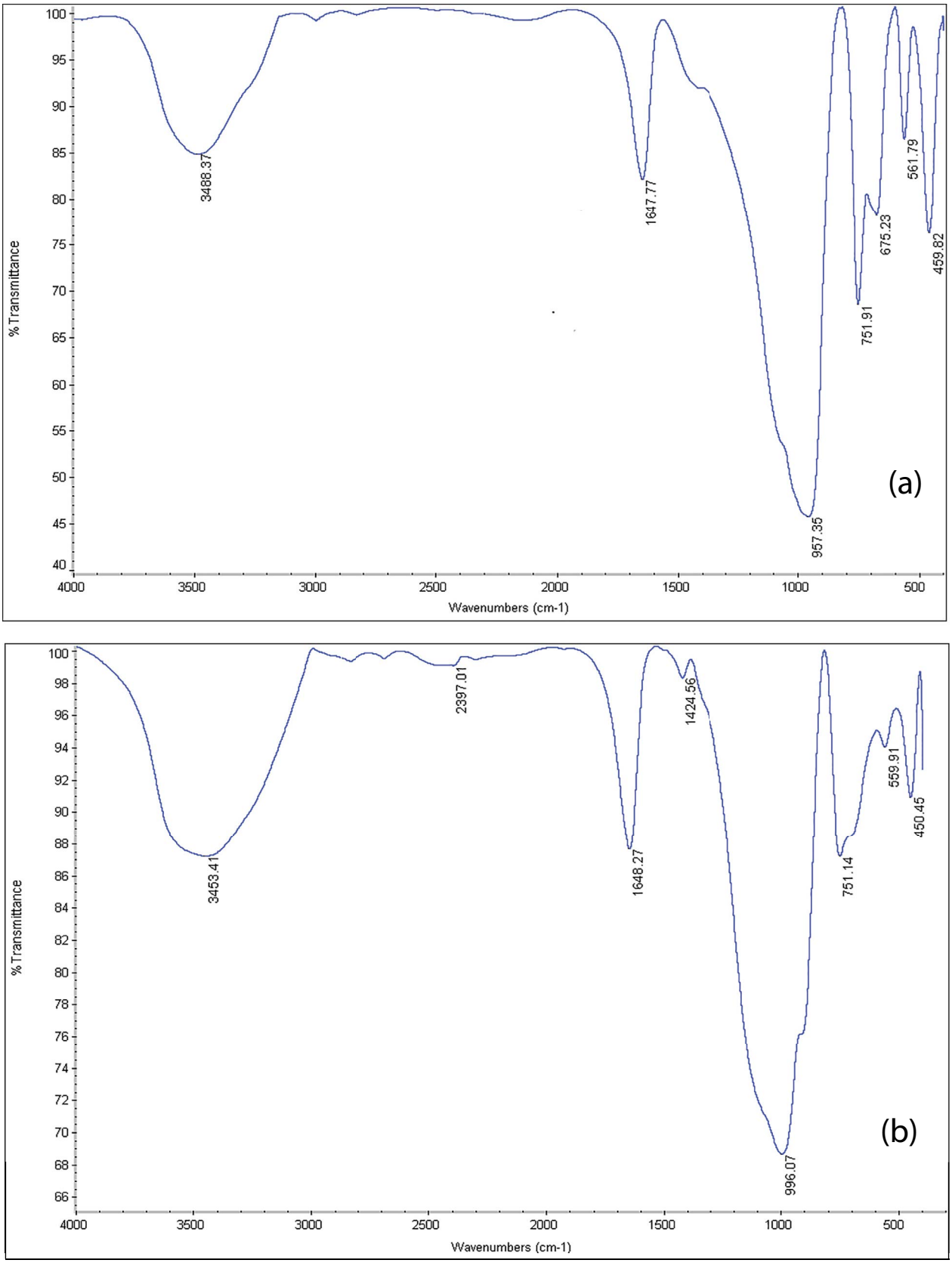

Fig. 4. FTIR spectrum of 13X zeolite (a) raw zeolite and (b) Cu modified zeolite.

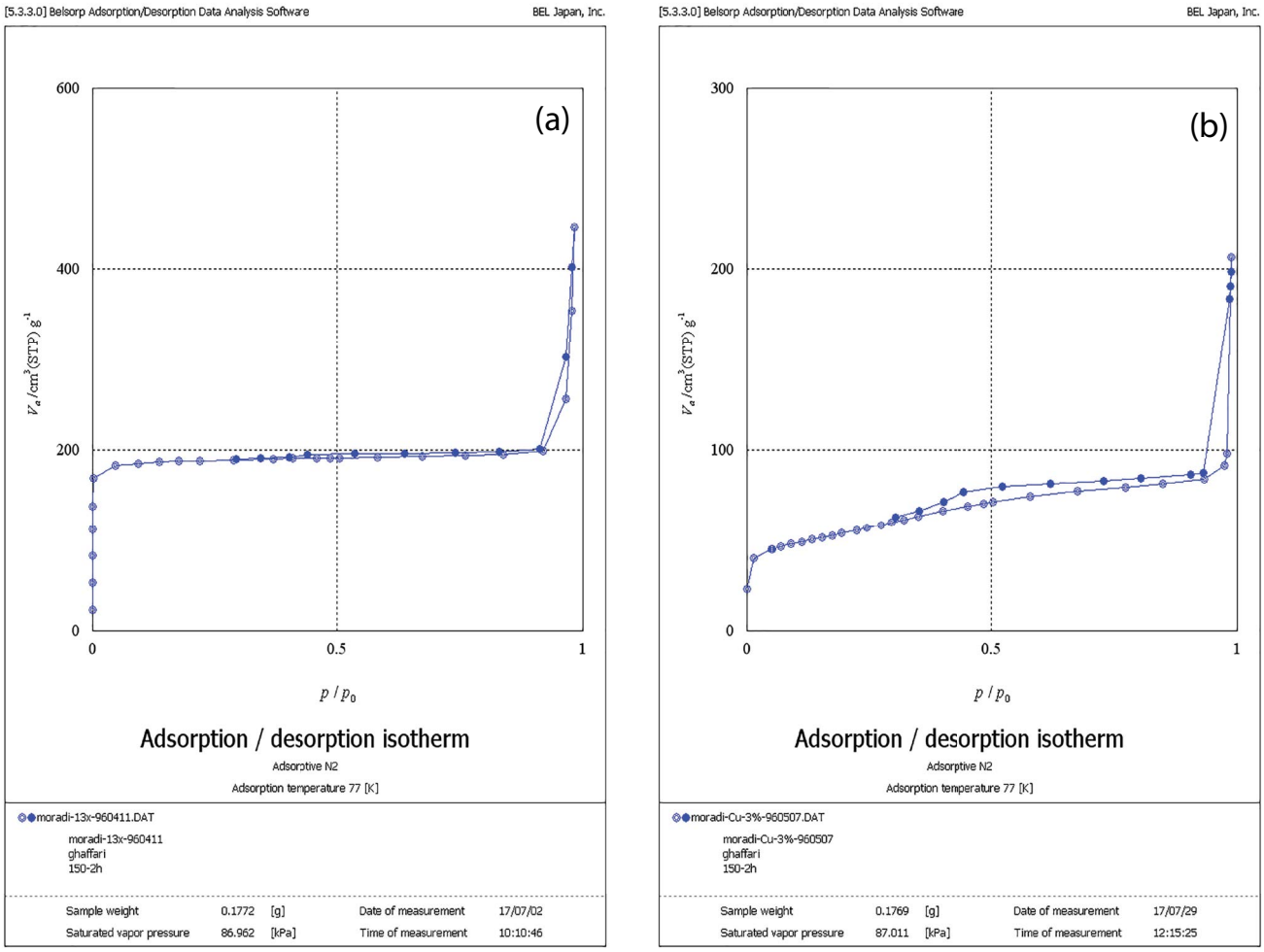

Fig. 5. N_2 adsorption–desorption isotherms 13X zeolite (a) raw zeolite and (b) Cu modified zeolite.

Table 2
BET results of 13X zeolite (raw zeolite and Cu modified zeolite)

Sample	S_{BET} (m^2/g)	V_t (cm^3/g)	W_d (nm)
Raw 13X	7.597	0.69	3.64
Modified 13X (3 wt.%)	1.89	0.32	6.77

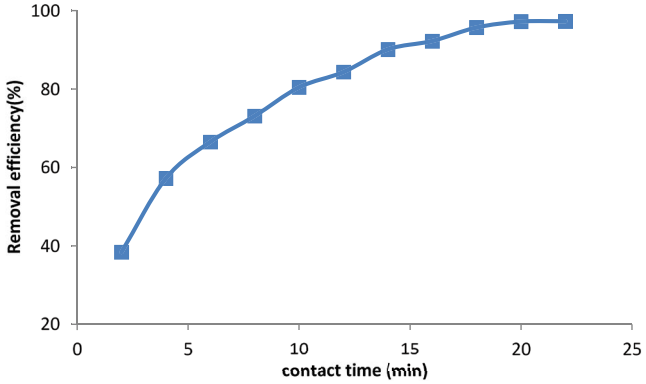

Fig. 6. Effect of contact time on the fenitrothion removal efficiency.

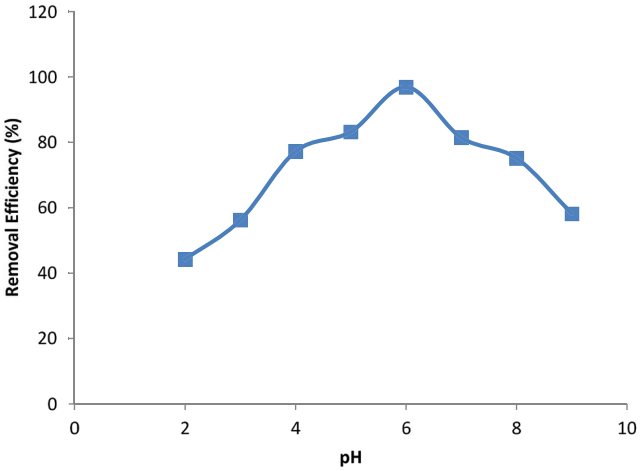

Fig. 7. Effect of pH on the fenitrothion removal efficiency.

the kinetic follows the pseudo-second-order at low concentration of pollutants [43]. The kinetic data also showed that the experimental data had a good harmony with the Morris–Weber equation, which shows that one of the other rate-limiting steps is the internal diffusion stage.

3.4. Effect of adsorbent dosage

In order to investigate the effect of adsorbent on the removal efficiency of fenitrothion by modified 13X zeolite, different amounts of adsorbents (0.05–0.3 g), in different experiments with the initial concentration, pH, optimum contact time and temperature of 50 mg/L, 6, 20 min and 20°C respectively were used. The results are presented in Fig. 8. It was observed that with increasing adsorbent, the removal efficiency increases. Hence, 0.2 g of modified 13X was selected as the optimum amount of adsorbent, and the same amount of adsorbent was used in the next experiments. Increasing adsorption efficiency by increasing the amount of adsorbent can be explained in such a way that by increasing the adsorbent, more sites (for a certain amount of absorbent) are provided, so the absorption efficiency is expected to increase. At the same time, after increasing the amount of adsorbent (modified 13X to 0.2 g) since the amount of absorbance is constant (50 mg/L), so although adsorbent sites have been increased, overall, the absorption rate due to the constant because the amount of adsorbate (fenitrothion) does not increase [49].

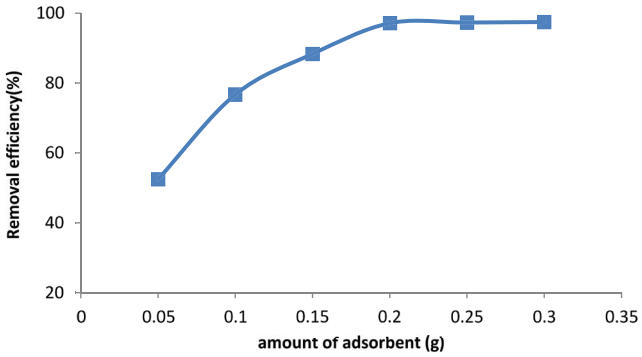

Fig. 8. Effect of amount of adsorbent on the fenitrothion removal efficiency.

3.5. Effect of initial concentration of fenitrothion on the adsorption

To investigate the effect of initial concentration on the adsorption process, various concentrations of aqueous fenitrothion solution were prepared and the adsorption process was performed under optimal conditions for the uptake of fenitrothion onto modified 13X at a concentrations range of 50–225 mg/L (Fig. 9). As it is seen, by increasing the concentration of fenitrothion in the solution, the absorption capacity has been reduced. To justify this, these active sites on the surface of the adsorbent have a constant value, and when the concentration increases, these sites are occupied and the absorption capacity decreases.

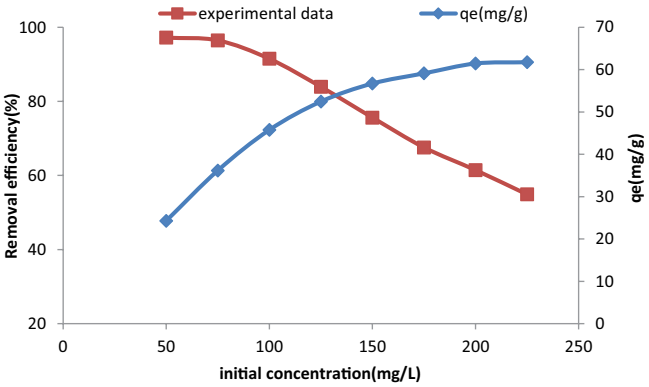

Fig. 9. Effect of initial concentration on the fenitrothion removal efficiency.

Table 3
Kinetic constants for fenitrothion adsorption

Morris–Weber equation [46,47]	K_{id} (min^{-1})	R^2	
$q_t = K_{id}t^{0.5} + C$	4.6897	0.9725	
Pseudo-first-order kinetic model [48]	K (min^{-1})	q_e (mg/g)	R^2
$\log(q_e - q_t) = \log q_e - \left(\frac{K}{2.303}\right)t$	0.1313	5.666	0.8253
Pseudo-second-order kinetic model [43]	k_2 (g mg^{-1} min^{-1})	q_e (mg/g)	R^2
Type 1: $\frac{t}{q_t} = \frac{1}{k_2 q_e^2} + \frac{1}{q_e}t$ $\frac{t}{q_t}$ vs t	7.31×10^{-3}	29.76	0.9976
Type 2: $\frac{1}{q_t} = \frac{1}{q_e} + \left(\frac{1}{k_2 q_e^2}\right)\frac{1}{t}$ $\frac{1}{q_t}$ vs $\frac{1}{t}$	8.9×10^{-3}	28.41	0.996
Type 3: $q_t = q_e - \left(\frac{1}{k_2 q_e}\right)\frac{q_t}{t}$ q_t vs $\frac{q_t}{t}$	8.4×10^{-3}	28.81	0.9812
Type 4: $\frac{q_t}{t} = k_2 q_e^2 - k_2 q_e (q_t)$ $\frac{q_t}{t}$ vs q_t	8.2×10^{-3}	28.99	0.9812

The results of Fig. 9 are used for isotherm computing, that is, Langmuir (four various linear types), Freundlich, Temkin and Dubnin–Randkovich (D–R).

3.6. Isotherm model

Absorption isotherm models generally show the amount of absorbed material in equilibrium as a function of the equilibrium concentration of the solution sorbed in a solution on a specific sorbent at a constant temperature. The most widely used isotherm models that are used to identify the absorption process mechanism are Langmuir and Freundlich models. Other isotherms such as D–R and Temkin are also used to determine the absorption energy and to obtain more information about the absorption mechanism. In this research, four isotherm models for describing the fenitrothion adsorption mechanism onto modified 13X are investigated. The details of isotherm models were presented in the previous work [43,45]. The fitted constants for the Langmuir (four various linear types), Freundlich, Temkin and D–R models along with regression coefficients are summarized in Table 4. From the regression coefficients (Table 2) it is found that the best fitting was obtained by the Langmuir-Type 1 compared to the other isotherm models. Also, results indicated that there was a good agreement between the experimental and predicted results in the following order Langmuir-Type 1 > Langmuir-Type 2 > Temkin > Langmuir-Type 3 > D–R > Langmuir-Type 4 > Freundlich.

3.7. Effect of temperature on adsorption of fenitrothion

The effect of temperature on the uptake of fenitrothion from aqueous solution was investigated at a temperature range of 20°C–50°C. The experiments were carried out under optimum conditions in the previous stages. The results are shown in Table 5. As the results show, the increase in temperature in the experiments carried out by the modified 13X absorbent decreased the removal efficiency of fenitrothion from an aqueous solution, although this amount is not significant. In justifying this, it can be said that as the temperature increases, the thickness of the boundary layer increases around the adsorbent, and therefore, the transfer of the absorbed component from the solution to the adsorbent active sites is more difficult, which leads to a decrease in the removal efficiency. Increasing the temperature can decrease the number of active sites available for sorption. The negative effect of the temperature on the removal efficiency indicates that the fenitrothion adsorption is exothermic.

Table 5
Effect of temperature on the removal efficiency

Temperature (°C)	Removal efficiency of fenitrothion (%)
20	97.01
30	94.67
40	87.24
50	75.83

Table 4
Isotherm constants for fenitrothion adsorption

			K_L (min^{-1})	q_m (mg/g)	R_L	R^2
Langmuir equation [50]	Type 1: $\frac{C_e}{q_e}=\frac{1}{(q_mK_L)}+\left(\frac{1}{q_m}\right)C_e$	$\frac{C_e}{q_e}$ vs C_e	0.322	63.29	0.0585–0.0136	0.9994
	Type 2: $\frac{1}{q_e}=\frac{1}{(q_mK_LC_e)}+\left(\frac{1}{q_m}\right)$	$\frac{1}{q_e}$ vs. $\frac{1}{C_e}$	0.488	60.61	0.0394–0.009	0.9876
	Type 3: $q_e=q_m-\left(\frac{1}{K_L}\right)\frac{q_e}{C_e}$	q_e vs. $\frac{q_e}{C_e}$	0.492	60.64	0.0391–0.009	0.9623
	Type 4: $\frac{q_e}{C_e}=K_lq_m-K_lq_e$	$\frac{q_e}{C_e}$ vs. q_e	0.474	61.07	0.0405–0.0093	0.9385
Freundlich equation [51]			K (min^{-1})	n	R^2	
$\log(q_e)=\log(K_F)+\frac{1}{n}\log C_e$			27.08	5.089	0.9126	
Temkin equation [52,53]			K_T	B	R^2	
$q_e=B\ln K_T+B\ln C_e$			21.6282	8.3485	0.9696	
D–R equation [54,55]			R^2	q_m	β	
$\ln q_e=\ln q_m-\beta\varepsilon^2$			8×10^{-8}	92.638	0.9564	
$\varepsilon=RT\ln\left(1+\frac{1}{C_e}\right)$						

Table 6
Thermodynamic parameter for adsorption of fenitrothion onto zeolite

ΔH (kJ/mol)	ΔS (kJ/mol K)	T (°C)	ΔG (kJ/mol)	R^2
–66.213	0.196	20	–8.4805	0.9932
		30	–7.2513	
		40	–5.0049	
		50	–3.0719	

3.8. Effect of temperature on thermodynamics parameter on adsorption of fenitrothion

Using the data in Table 5, the thermodynamics of absorption processes are discussed and various thermodynamic parameters such as the Gibbs free energy (ΔG), enthalpy (ΔH) and entropy (ΔS) parameters are calculated using Eqs. (4)–(6).

$$K_c = \frac{F_e}{1 - F_e} \tag{4}$$

$$\log K_c = \frac{-\Delta H}{2.303RT} + \frac{\Delta S}{2.303R} \tag{5}$$

$$\Delta G = -RT \ln K_c \tag{6}$$

where F_e is the fraction of fenitrothion sorbed at equilibrium. The values of these parameters are presented in Table 6. As the results are clear, the enthalpy variations (ΔH) are negative, which indicates that the adsorption reaction is exothermic. Also, the positive values of ΔS reveal that the solid phase and liquid phase interface increases randomly during the stabilization of the ions on the adsorbent surface. The negativity of ΔG values at all three temperatures also indicates that the fenitrothion adsorption reaction is self-contained in aqueous solutions at all three temperatures.

4. Conclusions

The modified 13X zeolite by copper nanoparticles (copper nanoparticles were coated on a bed of 13X), was used as an adsorbent for adsorption of fenitrothion from aqueous solutions in a batch process. The raw and modified 13X characterized by XRD, FTIR, SEM, EDX, and BET. These results show that the copper nanoparticles are well dispersed on the high surface 13X zeolite support by simple impregnation. The optimum conditions of fenitrothion sorption were found to be as follows: a sorbent dose of 0.2 g in 100 mL of solution and contact time 20 min. The kinetic data showed that the uptake process was controlled by a pseudo-second-order equation (Type-1). Results obtained from this study were well described by the theoretical Langmuir (Type-1). Thermodynamic studies demonstrated negative ΔG and ΔH and positive ΔS. Results showed the exothermic nature of the adsorption.

Acknowledgments

The authors would like to acknowledge Amol University of Special Modern Technologies for support and facilitation of this study.

References

[1] P.H. Howard, Handbook of Environmental Fate and Exposure Data: For Organic Chemicals, Volume III Pesticides, CRC press, Boca Raton, Florida, 1991.
[2] G.Z. Memon, M.I. Bhanger, M. Akhtar, F.N. Talpur, J.R. Memon, Adsorption of methyl parathion pesticide from water using watermelon peels as a low cost adsorbent, Chem. Eng. J., 138 (2008) 616–621.
[3] H.F. Shaalan, Treatment of pesticides containing effluents using organoclays/nanofiltration systems: rational design and cost indicators, Desal. Water Treat., 5 (2009) 153–158.
[4] M. Armaghan, M.M. Amini, Adsorption of diazinon and fenitrothion on MCM-41 and MCM-48 mesoporous silicas from non-polar solvent, Colloid J., 71 (2009) 583–588.
[5] M. Armaghan, M.M. Amini, Adsorption of diazinon and fenitrothion on nanocrystalline magnesium oxides, Arabian J. Chem., 10 (2017) 91–99.
[6] Y. Nakaoka, H. Katsumata, S. Kaneco, T. Suzuki, K. Ohta, Photocatalytic degradation of diazinon in aqueous solution by platinized TiO_2, Desal. Water Treat., 13 (2010) 427–436.
[7] L. Sarabia, I. Maurer, E. Bustos-Obregón, Melatonin prevents damage elicited by the organophosphorous pesticide diazinon on mouse sperm DNA, Ecotoxicol. Environ. Saf., 72 (2009) 663–668.
[8] H.M. Dutta, D. Misquitta, S. Khan, The effects of endosulfan on the testes of bluegill fish, *Lepomis macrochirus*: a histopathological study, Arch. Environ. Contam. Toxicol., 51 (2006) 149–156.
[9] P. Moudgil, A. Gupta, A. Sharma, S. Gupta, A. Tiwary, Potentiation of spermicidal activity of 2′,4′-dichlorobenzamil by lidocaine, Indian J. Exp. Biol., 40 (2002) 1373–1377.
[10] M. Yousef, F.E. Demerdash, K.A. Salhen, Protective role of isoflavones against the toxic effect of cypermethrin on semen quality and testosterone levels of rabbits, J. Environ. Sci. Health., Part B, 38 (2003) 463–478.
[11] F. Kamel, A.S. Rowland, L.P. Park, W.K. Anger, D.D. Baird, B.C. Gladen, T. Moreno, L. Stallone, D.P. Sandler, Neurobehavioral performance and work experience in Florida farmworkers, Environ. Health Perspect., 111 (2003) 1765–1772.
[12] J.A. Firestone, T.S. Weller, G. Franklin, P. Swanson, W. Longstreth, H. Checkoway, Pesticides and risk of Parkinson disease: a population-based case-control study, Arch. Neurol., 62 (2005) 91–95.
[13] L. Ezemonye, T. Ikpesu, I. Tongo, Distribution of diazinon in water, sediment and fish from Warri River, Niger Delta, Nigeria, Jordan, J. Biol. Sci., 1 (2008) 77–83.
[14] A.B. Couso, D.F. Calviño, M.P. Moure, J.C.N. Muñoz, J.S. Gándara, M.A. Estévez, Adsorption and desorption kinetics of carbofuran in acid soils, J. Hazard. Mater., 190 (2011) 159–167.
[15] B.J. Johnson, A.P. Malanoski, I.A. Leska, B.J. Melde, J.R. Taft, M.A. Dinderman, J.R. Deschamps, Adsorption of organophosphates from solution by porous organosilicates: capillary phase-separation, Microporous Mesoporous Mater., 195 (2014) 154–160.
[16] M. Brigante, M. Avena, Synthesis, characterization and application of a hexagonal mesoporous silica for pesticide removal from aqueous solution, Microporous Mesoporous Mater., 191 (2014) 1–9.
[17] M.I. Badawy, M.Y. Ghaly, T.A.G. Allah, Advanced oxidation processes for the removal of organophosphorus pesticides from wastewater, Desalination, 194 (2006) 166–175.
[18] Y. Sun, J.J. Pignatello, Photochemical reactions involved in the total mineralization of 2,4-D by iron (3+)/hydrogen peroxide/UV, Environ. Sci. Technol., 27 (1993) 304–310.

[19] O.M. Alfano, R.J. Brandi, A.E. Cassano, Degradation kinetics of 2,4-D in water employing hydrogen peroxide and UV radiation, Chem. Eng. J., 82 (2001) 209–218.
[20] W. Chu, Modeling the quantum yields of herbicide 2,4-D decay in UV/H_2O_2 process, Chemosphere, 44 (2001) 935–941.
[21] R.J. Wu, C.C. Chen, C.S. Lu, P.Y. Hsu, M.H. Chen, Phorate degradation by TiO_2 photocatalysis: parameter and reaction pathway investigations, Desalination, 250 (2010) 869–875.
[22] M. Trillas, J. Peral, X. Domènech, Redox photodegradation of 2,4-dichlorophenoxyacetic acid over TiO_2, Appl. Catal., B, 5 (1995) 377–387.
[23] M. Trillas, J. Peral, X. Domenech, Photocatalyzed degradation of phenol, 2,4-dichlorophenol, phenoxyacetic acid and 2,4-dichlorophenoxyacetic acid over supported TiO_2 in a flow system, J. Chem. Technol. Biotechnol., 67 (1996) 237–242.
[24] E. Brillas, J.C. Calpe, J. Casado, Mineralization of 2,4-D by advanced electrochemical oxidation processes, Water Res., 34 (2000) 2253–2262.
[25] E. Brillas, R. Sauleda, J. Casado, Degradation of 4-chlorophenol by anodic oxidation, electro-fenton, photoelectro-Fenton, and peroxi-coagulation processes, J. Electrochem. Soc., 145 (1998) 759–765.
[26] P. Pillewan, S. Mukherjee, A.K. Meher, S. Rayalu, A. Bansiwal, Removal of arsenic(III) and arsenic(V) using copper exchange zeolite-A, Environ. Prog. Sustainable Energy, 33 (2014) 1274–1282.
[27] S. Salvestrini, P. Vanore, P. Iovino, V. Leone, S. Capasso, Adsorption of simazine and boscalid onto acid-activated natural clinoptilolite, Environ. Eng. Manage. J., 14 (2015) 1705–1712.
[28] R.E. Apreutesei, C. Catrinescu, C. Teodosiu, Studies regarding phenol and 4-chlorophenol sorption by surfactant modified zeolites, Environ. Eng. Manage. J., 8 (2009) 651–656.
[29] E. Fuentes, M.E. Báez, R. Labra, Parameters affecting microwave-assisted extraction of organophosphorus pesticides from agricultural soil, J. Chromatogr. A, 1169 (2007) 40–46.
[30] W. Baarschers, J. Elvish, S. Ryan, Adsorption of fenitrothion and 3-methyl-4-nitrophenol on soils and sediment, Bull. Environ. Contam. Toxicol., 30 (1983) 621–627.
[31] G.M. Lule, M.U. Atalay, Comparison of fenitrothion and trifluralin adsorption on organo-zeolites and activated carbon. Part II: thermodynamic parameters and the suitability of the kinetic models of pesticide adsorption, Part. Sci. Technol., 32 (2014) 426–430.
[32] B. Bowman, W. Sans, Adsorption of parathion, fenitrothion, methyl parathion, aminoparathion and paraoxon by Na+, Ca^{2+}, and Fe^{3+} montmorillonite suspensions, Soil Sci. Soc. Am. J., 41 (1977) 514–519.
[33] J.S. Lee, J.H. Kim, J.T. Kim, J.K. Suh, J.M. Lee, C.H. Lee, Adsorption equilibria of CO_2 on zeolite 13X and zeolite X/activated carbon composite, J. Chem. Eng. Data, 47 (2002) 1237–1242.
[34] H. Zhang, Y. Wang, P. Bai, X. Guo, Adsorption of Acetic Acid from Dilute Solution on Zeolite 13X: Isotherm, Kinetic and Thermodynamic Studies, Proceedings of 3rd International Conference on Application of Materials Science and Environmental Materials (AMSEM2015), World Scientific, Phuket Island, Thailand, 2016, pp. 40–47.
[35] L.Z. Melgar, S. Machado, Determination of fenitrothion in commercial formulations by square wave voltammetry and UV-Vis spectroscopy, J. Braz. Chem. Soc., 16 (2005) 743–748.
[36] H. Esfandian, V. Garshasbi, Investigation of methane adsorption on molecular sieve zeolite (from natural materials), Gas Process. J., 8 (2020) 35–50.
[37] Y. Ma, C. Yan, A. Alshameri, X. Qiu, C. Zhou, Synthesis and characterization of 13X zeolite from low-grade natural kaolin, Adv. Powder Technol., 25 (2014) 495–499.
[38] T.Z. Ren, Z.Y. Yuan, B.L. Su, Surfactant-assisted preparation of hollow microspheres of mesoporous TiO_2, Chem. Phys. Lett., 374 (2003) 170–175.
[39] A.S. Maybodi, S.M. Pourali, Microwave-assisted aging synthesis of bismuth modified zeolite-P microspheres via BiOCl nanoflake transformation, Microporous Mesoporous Mater., 167 (2013) 127–132.
[40] K.H. Schnabel, G. Finger, J. Kornatowski, E. Löffler, C. Peuker, W. Pilz, Decomposition of template in SAPO-5 and AlPO 4-5 molecular sieves studied by IR and Raman spectroscopy, Microporous Mater., 11 (1997) 293–302.
[41] G. Sánchez, B. Dlugogorski, E. Kennedy, M. Stockenhuber, Zeolite-supported iron catalysts for allyl alcohol synthesis from glycerol, Appl. Catal., A, 509 (2016) 130–142.
[42] T. Mehta, A. Rathi, A. Verma, S. Barman, G. Halder, Elimination of Fipronil insecticide by adsorption technique from aqueous solution by Cu-13X zeolite composite: isotherms, kinetic and thermodynamic studies, Int. J. Environ. Anal. Chem., (2020) 1–17, doi: 10.1080/03067319.2020.1790545.
[43] H. Esfandian, A.S. Maybodi, M. Parvini, B. Khoshandam, Development of a novel method for the removal of diazinon pesticide from aqueous solution and modeling by artificial neural networks (ANN), J. Ind. Eng. Chem., 35 (2016) 295–308.
[44] P. Mondal, B. Mohanty, C.B. Majumder, Removal of arsenic from simulated groundwater using GAC-Ca in batch reactor: kinetics and equilibrium studies, Clean–Soil Air Water, 40 (2012) 506–514.
[45] H. Esfandian, S.G. Pakdehi, M.J. Cattallany, Development of a novel method for sodium azide removal from aqueous solution using amberlite IRA-900: batch and column adsorption studies, Desal. Water Treat., 193 (2020) 381–391.
[46] H. Esfandian, M. Parvini, B. Khoshandam, A.S. Maybodi, Artificial neural network (ANN) technique for modeling the mercury adsorption from aqueous solution using *Sargassum Bevanom* algae, Desal. Water Treat., 57 (2016) 1–14.
[47] W.J. Weber, J.C. Morris, Kinetics of adsorption on carbon from solution, J. Sanit. Eng. Div., 89 (1963) 31–60.
[48] R.H. Chen, H.T. Qiao, Y. Liu, Y.H. Dong, P. Wang, Z. Zhang, T. Jin, Adsorption of methylene blue from an aqueous solution using a cucurbituril polymer, Environ. Prog. Sustainable Energy, 34 (2015) 512–519.
[49] A. Shukla, Y.H. Zhang, P. Dubey, J. Margrave, S.S. Shukla, The role of sawdust in the removal of unwanted materials from water, J. Hazard. Mater., 95 (2002) 137–152.
[50] I. Langmuir, The adsorption of gases on plane surfaces of glass, mica and platinum, J. Am. Chem. Soc., 40 (1918) 1361–1403.
[51] H. Freundlich, Of the adsorption of gases. Section II. Kinetics and energetics of gas adsorption. Introductory paper to section II, Trans. Faraday Soc., 28 (1932) 195–201.
[52] M. Temkin, V. Pyzhev, Recent modifications to Langmuir isotherms, Acta Phys. Chim. Sin., 12 (1940) 217–222.
[53] P.K. Raul, R.R. Devi, I.M. Umlong, A.J. Thakur, S. Banerjee, V. Veer, Iron oxide hydroxide nanoflower assisted removal of arsenic from water, Mater. Res. Bull., 49 (2014) 360–368.
[54] M. Dubinin, L. Radushkevich, Equation of the characteristic curve of activated charcoal, Chem. Zentr., 1 (1947) 875.
[55] R. Katal, H. Pahlavanzadeh, Zn(II) ion removal from aqueous solution by using a polyaniline composite, J. Vinyl Add. Tech., 17 (2011) 138–145.